engineering proceedings

Proceeding Paper

A Soft Robot Arm with Flexible Sensors for Master–Slave Operation †

Yoshie Yamamoto, Shuichi Wakimoto *, Takefumi Kanda and Daisuke Yamaguchi

Graduate School of Natural Science and Technology, Okayama University, Okayama 700-8530, Japan; yamamoto19@s.okayama-u.ac.jp (Y.Y.); kanda-t@okayama-u.ac.jp (T.K.); yamaguchi20@okayama-u.ac.jp (D.Y.)
* Correspondence: wakimoto@okayama-u.ac.jp; Tel.: +81-86-251-8105

† Presented at 8th International Electronic Conference on Sensors and Applications, 1–15 November 2021; Available online: https://ecsa-8.sciforum.net.

Abstract: In our study, a soft robot arm consisting of McKibben artificial muscles and a silicone rubber structure was developed. This robot arm can perform bending and twisting motions by ap-plying pneumatic pressure to the artificial muscles. The robot arm is made of flexible materials only, and therefore it has high flexibility and shape adaptability. In this report on the fundamental investigation of the master–slave feedback control of the soft robot arm for intentional operation, we focus on the bending motion of the soft robot arm. Three flexible strain sensors were placed on the soft robot arm for measuring the bending motion. By establishing a master–slave feedback system using the sensors, the bending motion of the soft robot arm followed the operator's wrist motion detected via the wearable interface device.

Keywords: soft robot arm; artificial muscle; flexible strain sensor; master–slave control

check for updates

Citation: Yamamoto, Y.; Wakimoto, S.; Kanda, T.; Yamaguchi, D. A Soft Robot Arm with Flexible Sensors for Master–Slave Operation. *Eng. Proc.* **2021**, *10*, 34. https://doi.org/10.3390/ecsa-8-11311

Academic Editor: Stefano Mariani

Published: 1 November 2021

1. Introduction

In recent years, various soft actuators have attracted much attention due to their high compliance, light weight, and power-to-weight ratio. In addition, research on soft robot arms using these actuators has been actively conducted [1–6]. Due to their high flexibility and back-drivability, these soft robot arms can absorb the impact of collisions with people or objects and minimize the impact on the target. Therefore, the soft robot arm has better safety than conventional robot arms, which are composed of rigid mechanical elements.

The McKibben artificial muscle used in this study is one of the most widely known soft actuators [7]. It contracts like a real muscle when pneumatic pressure is applied. In our research group, a soft robot arm with multiple McKibben artificial muscles has been developed. The robot arm can perform bending and twisting motions [8]. Due to its flexibility and safety, it is expected to be applicable to mechanical systems in medical, welfare, and agricultural fields.

In these fields, unlike for general industrial robot arms, where predetermined motions are repeated at high speed based on high-precision positioning control, the operator's intention needs to be reflected flexibly in the motions of the robot arm, depending on the situation and task. For intentional operation, research has been conducted on master–slave control using a manipulation interface that is similar to that of the robot arm, and on remote control using human motions through wearable devices [9–12]. In this study, we have developed an arm-mounted wearable interface with thin flexible strain sensors attached to a highly elastic arm cover. The interface detects the flexion of the operator's wrist and the twist of the operator's forearm, and these are used as inputs for the bending and twisting motions of the soft robotic arm, respectively. This enables intuitive operation of the soft robot arm [10]. In order to reflect the operator's intention more efficiently in the motion of the soft robotic arm, it is effective to introduce feedback control to the master–slave operation.

In this paper, we focus on the bending motion as a basic research study to realize the feedback control. Three flexible strain sensors were mounted on the soft robot arm for feedback control of its bending motion. These sensors corresponded in a one-to-one fashion to the three sensors of the wearable interface that respond to the bending of the wrist. Feedback control of the bending motion of the soft robot arm was realized by comparing the corresponding sensor values.

2. Materials and Methods

2.1. Components and Structure of a Soft Robot Arm

2.1.1. McKibben Artificial Muscle

The general McKibben artificial muscle consists of a rubber tube covered with a sleeve made of woven nylon fibers. The rubber tube is sealed at one end, and an air supply tube is connected to the other end. The driving principle of the McKibben artificial muscle is shown in Figure 1. By applying air pressure from an air supply tube, the inner rubber tube expands in the radial direction, and a contractile displacement in the axial direction is generated by changing the braid angle of the sleeve. The contraction motion is used as the output of the actuator.

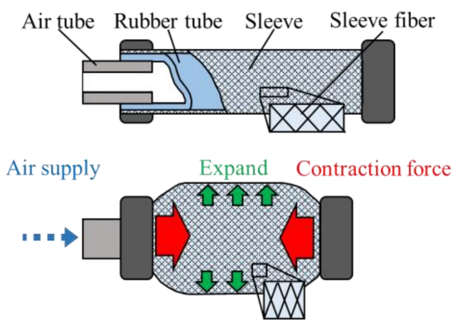

Figure 1. Structure and driving principle of the McKibben artificial muscle.

2.1.2. Flexible Strain Sensor

Figure 2 shows an overview of the flexible strain sensor (stretchable dynamic strain sensor, Yamaha Corporation) used in this study. The sensor consists of an electric conductive CNT (carbon nanotube) sheet sandwiched between elastic polymer layers with electrodes attached to both ends. It is flexible, and when strain occurs in the direction of the CNT array, the electrical resistance increases, and this change in electrical resistance is used as the output of the sensor to measure the strain. The thickness, the gauge length, and the width of the sensor are 0.2 mm, 90 mm, and 2.0 mm, respectively.

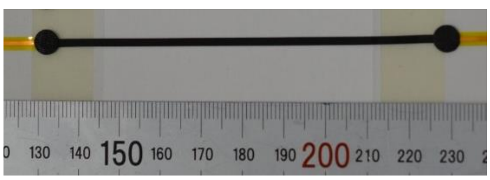

Figure 2. Overview of the flexible strain sensor.

2.1.3. Structure of a Soft Robot Arm

Figure 3 shows a model of the soft robot arm developed in our study. The robot arm consists of five McKibben artificial muscles. The robot arm was fabricated by placing the artificial muscles in a mold and then pouring liquid rubber into the mold before hardening. Three artificial muscles, which are represented as red lines in Figure 3, were placed at equal intervals in parallel to at the axial direction, and these generate the bending motion of the soft robot arm. Two artificial muscles, which are shown as green lines in Figure 3, were wound spirally, one in the clockwise direction and the other in the counterclockwise direction. These enable the robot arm to twist. Table 1 shows the parameters of the robot arm.

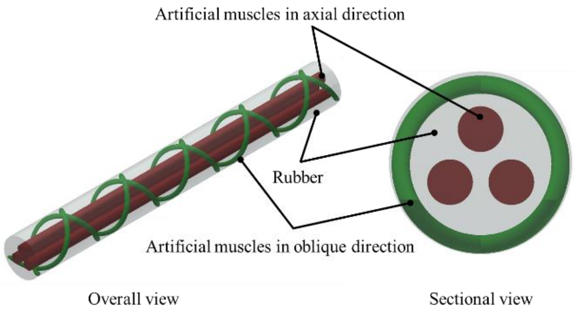

Figure 3. Structure of the soft robot arm.

Table 1. Parameters of the robot arm.

Robot arm	Overall length [mm] Outer diameter [mm]	190 22
Artificial muscles in the axial direction	Length [mm] Outer diameter [mm]	180 5.5
Artificial muscles in the clockwise and counterclockwise directions	Length [mm] Outer diameter [mm] Number of rolls [times]	350 2.5 5
Rubber material	Hardness	30 (durometer OO)

2.1.4. Mounting Flexible Strain Sensors on a Soft Robot Arm

Figures 4 and 5 indicate the layout and the actual placement of the sensors. In this study, focusing on the feedback control of the bending motion of the soft robot arm, three flexible strain sensors (rs_1, rs_2, and rs_3) were attached on the surface of the soft robot arm at 120° intervals in the axial direction to match each artificial muscle with a one-to-one correspondence. The sensors (rs_1, rs_2, and rs_3) and artificial muscles (ra_1, ra_2, and ra_3) were arranged opposite to each other in pairs, so that when the artificial muscle contracts, the corresponding sensor is stretched, and the electrical resistance increases.

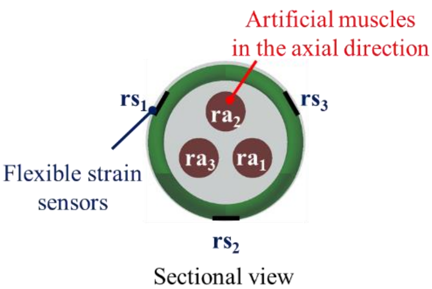

Figure 4. Layout of the sensors on the soft robot arm.

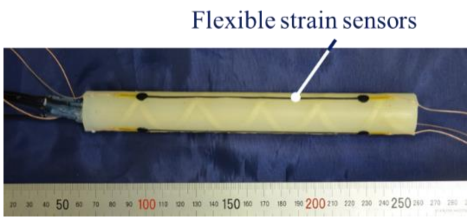

Figure 5. The flexible strain sensors on the soft robot arm.

2.2. Structure of a Wearable Interface

A wearable interface, as shown in Figure 6, was developed in previous research [13]. It was fabricated by attaching flexible strain sensors to a stretchable arm cover. To detect the bending motion of the wrist, three sensors (ws_1, ws_2, and ws_3) were placed at equal intervals in the axial direction at the wrist. In addition, two sensors (ws_4 and ws_5) were placed crosswise on the forearm to detect the twisting motion of the forearm. In this study, three sensors in the axial direction were used because only the bending of the wrist was targeted in this basic study.

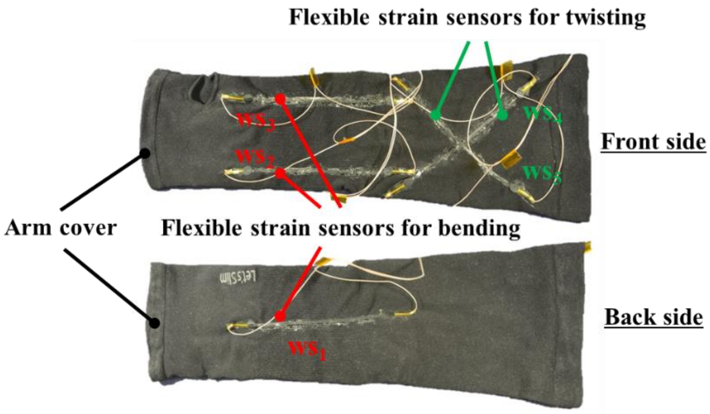

Figure 6. Wearable interface [13].

3. Experiments and Results

Feedback Control of Bending Motion

The correspondences between the sensors of the wearable interface and those of the soft robot arm are shown in Figure 7. The block diagram of the feedback control system is shown in Figure 8. The sensor outputs of three sensors on the wearable interface change with the bending of the operator's wrist. The deviation E is the difference between the change in the electrical resistance R_{wsi} (i = 1, 2, 3) and the change in the resistance R_{rsi} (i = 1, 2, 3) of the three sensors on the soft robot arm. The feedback gain of K_{i} (i = 1, 2, 3) was set so that R_{wsi} at the maximum wrist bending matched $K_{\mathrm{i}}R_{\mathrm{rsi}}$ at the maximum bending of the robot arm. P_{i} (i = 1, 2, 3) is the actuating pneumatic pressure value for the artificial muscles. The size and motion ranges of wrists differ from one person to another. In addition, the position and the tightness of the wearable interface on the arm vary slightly each time an operator wears the interface, even for the same operator. Therefore, K_{i} needs to be adjusted for each time of wearing before the feedback control experiment. The proportional gain and the integral gain of the PI controller were determined experimentally.

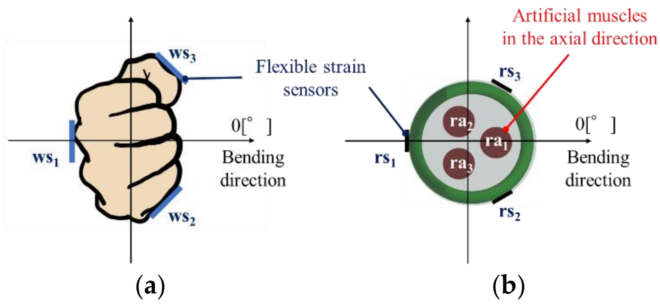

Figure 7. The correspondences between the sensors of the wearable interface and those of the soft robot arm (cross-sectional views): (**a**) operator's wrist; (**b**) soft robot arm.

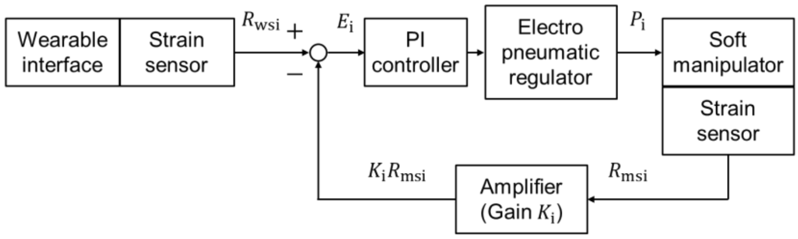

Figure 8. The system configuration for feedback control.

The operator with the wearable interface bent the wrist with a bending direction of 0° and extended it back to its initial state. The control results, without load and with a load of 10 g mass on the tip of the robot arm, are shown in Figures 9 and 10, respectively. In these graphs, we focus on R_{ws1} and R_{rs1}, because the bending direction is 0° and it is mainly R_{ws1} and R_{rs1} that change. Figures 9a and 10a show R_{wsi}, $K_i R_{rsi}$, and P_i. Figures 9b and 10b represent the comparison of the ratio of the bending angle to the maximum bending angle of the wrist and the robot arm. The maximum angles of the wrist and the robot arm are different, so the ratios of the bending angle to the maximum bending angle are compared. The bending angles of the wrist and robot arm were calculated by the motion capture system.

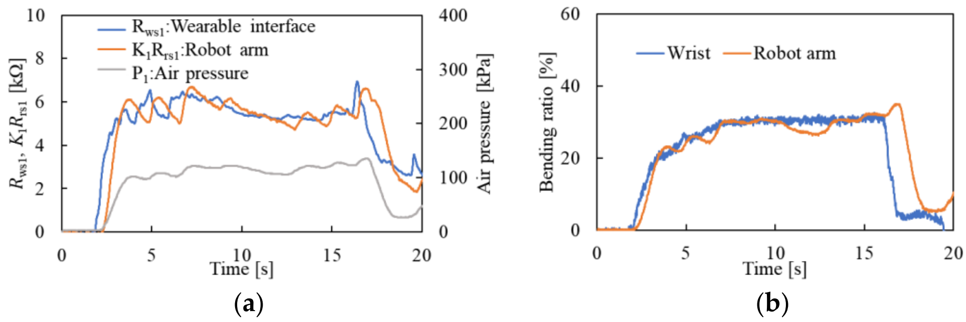

Figure 9. Control results without load. (**a**) Relation between R_{ws1}, $K_1 R_{rs1}$, and P_1; (**b**) comparison of bending ratios between the wrist and the robot arm.

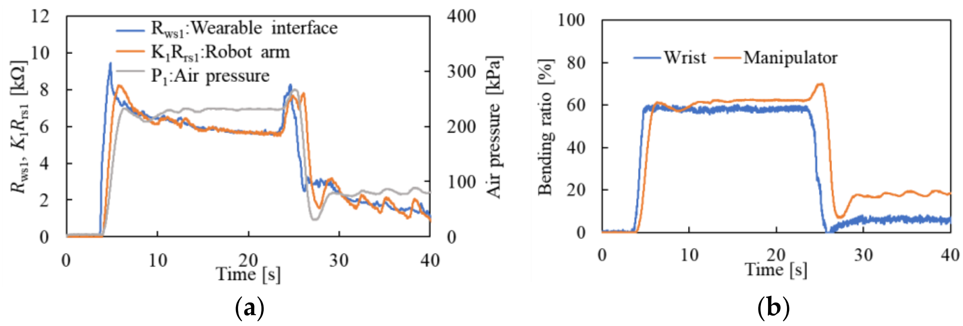

Figure 10. Control results with load. (**a**) Relation between R_{ws1}, $K_1 R_{rs1}$, and P_1; (**b**) comparison of bending ratios between the wrist and the robot arm.

As shown in Figures 9 and 10, $K_1 R_{rs1}$ follows R_{ws1} in both cases (without load and with load); therefore, it is found that a feedback control system with a PI controller works well. Moreover, the bending angle of the arm can follow the bending angle of the wrist to a great extent. Figures 9b and 10b show that the average error of the wrist and manipulator in the stable bending state is 1.4 % (from 3.4 s to 16.1 s) without load and 3.2 % (from 5.9 s to 23.5 s) with load. However, there is a delay of about 1.6 s in returning from the bending state to the initial state, both without and with load. This is due to the small exhaust flow rate. Furthermore, a steady-state error after returning from the bending state to the initial state can be observed in Figure 10b. This is caused by the mechanical misalignment between the wearable interface and the wrist, before and after the motion.

Generally, soft strain sensors made of polymer materials have a drift characteristic, where the sensor value fluctuates slightly even when the amount of strain is kept constant. In fact, this characteristic is observed to a slight extent in our devices. However, by using the difference in the soft sensor's outputs between the interface and the soft robot arm, the drift fluctuations of both sensors are almost canceled out, and master–slave feedback control is possible.

4. Conclusions

In this study, flexible strain sensors were attached onto the soft robot arm. A wearable interface was used to detect the wrist movement of the operator, and feedback control was used to make the robot arm follow the movement of the wrist. As a result, it was confirmed that the robot arm was controlled well for bending motion in a specific direction. This robot arm can perform bending and twisting motions. Therefore, we intend to apply the master–slave feedback control system to bending in any direction and to twisting motions, to verify the operability.

Supplementary Materials: The following are available online at https://www.mdpi.com/article/10.3390/ecsa-8-11311/s1.

Author Contributions: Conceptualization, S.W.; data curation, Y.Y.; funding acquisition, S.W.; investigation, Y.Y.; methodology, S.W., Y.Y., T.K. and D.Y.; writing, Y.Y. and S.W. All authors have read and agreed to the published version of the manuscript.

Funding: This research was funded by Japan Society for Promotion of Science, Grants-in-Aid for Scientific Research, Grant Number 20K04240.

Institutional Review Board Statement: Not applicable.

Informed Consent Statement: Not applicable.

Data Availability Statement: Not applicable.

Conflicts of Interest: The authors declare no conflict of interest.

References

1. Trivedi, D.; Dienno, D.; Rahn, C.D. Optimal, Model-Based Design of Soft Robotic Manipulators. *ASME J. Mech. Des.* **2008**, *130*, 091402-1–091402-9. [CrossRef]
2. Laschi, C.; Cianchetti, M.; Mazzolai, B.; Margheri, L.; Follador, M.; Dario, P. Soft Robot Arm Inspired by the Octopus. *Adv. Robot.* **2012**, *26*, 709–727. [CrossRef]
3. Ramses, V.M.; Jamie, L.B.; Carina, R.F.; Lihua, J.; Robert, F.S.; Rui, M.D.N.; Zhigang, S.; George, M.W. Robotic Tentacles with Three-Dimensional Mobility Based on Flexible Elastomers. *Adv. Mater.* **2012**, *25*, 205–212.
4. Yang, D.; Xu, M.; Li, W.; Zhang, S. Design and Implementation of a Soft Robotic Arm Driven by SMA Coils. *IEEE Trans. Ind. Electron.* **2019**, *66*, 6108–6116. [CrossRef]
5. Wang, H.; Zhang, R.; Chen, W.; Wang, X.; Pfeifer, R. A cable-driven soft robot surgical system for cardiothoracic endoscopic surgery: Preclinical tests in animals. *Surg. Endosc.* **2016**, *31*, 3152–3158. [CrossRef] [PubMed]
6. Ansari, Y.; Manti, M.; Falotico, E.; Cianchetti, M.; Laschi, C. Multiobjective Optimization for Stiffness and Position Control in a Soft Robot Arm Module. *IEEE Robot. Autom. Lett.* **2018**, *3*, 108–115. [CrossRef]
7. Schulte, H.F. The Characteristics of the McKibben Artificial Muscle. In *The Application of External Power in Prosthetics and Orthotics*; National Academy of Science-National Research Council: Washington, DC, USA, 1961; pp. 94–115.
8. Doi, T.; Wakimoto, S.; Suzumori, K.; Mori, K. Proposal of Flexible robotic arm with thin McKibben actuators mimicking octopus arm structure. In Proceedings of the 2016 IEEE/RSJ International Conference on Intelligent Robots and Systems (IROS), Daejeon, Korea, 9–14 October 2016.
9. Aliff, M.; Dohta, S.; Akagi, T.; Li, H. Development of a simple-structured pneumatic robot arm and its control using low-cost embedded controller. *Procedia Eng.* **2012**, *41*, 134–142. [CrossRef]
10. Furukawa, S.; Wakimoto, S.; Kanda, T.; Hagihara, H. A Soft Master-Slave Robot Mimicking Octopus Arm Structure Using Thin Artificial Muscles and Wire Encoders. *Actuators* **2019**, *8*, 40. [CrossRef]
11. Frazelle, C.G.; Kapadia, A.; Walker, I. Developing a Kinematically Similar Master Device for Extensible Continuum Robot Manipulators. *ASME J. Mech. Des.* **2018**, *10*, 025005-1–025005-8. [CrossRef]

12. Lim, S.; Son, D.; Kim, J.; Lee, Y.B.; Song, J.; Choi, S.; Lee, D.J.; Kim, J.H.; Lee, M.; Hyeon, T.; et al. Transparent and Stretchable Interactive Human Machine Interface Based on Patterned Graphene Heterostructures. *Adv. Funct. Mater.* **2014**, *25*, 375–383. [CrossRef]
13. Hagihara, H.; Wakimoto, S.; Kanda, T.; Furukawa, S. Operation of a pneumatic soft manipulator using a wearable interface with flexible strain sensors. In Proceedings of the 2019 IEEE/RSJ International Conference on Intelligent Robots and Systems (IROS), Macau, China, 3–8 November 2019.